analytical chemistry

Article

pubs.acs.org/ac

Unexpected Electrophoretic Behavior of Complexes between Rod-like Virions and Bivalent Antibodies

Stanislav S. Beloborodov,[†] Vasily G. Panferov,[‡] Irina V. Safenkova,[‡] Svetlana M. Krylova,[†] Boris B. Dzantiev,[‡] and Sergey N. Krylov*[,†]

[†]Department of Chemistry and Centre for Research on Biomolecular Interactions, York University, Toronto, Ontario M3J 1P3, Canada

[‡]A.N. Bach Institute of Biochemistry, Research Center of Biotechnology, Russian Academy of Sciences, Moscow 119071, Russia

Supporting Information

ABSTRACT: Here we report on the unexpected electrophoretic behavior of complexes between rod-like virus particles (virions) and bivalent antibodies. The multiple complexes formed by the virions and antibodies migrated with electrophoretic mobilities of much greater absolute values than those of the unbound virions or antibodies while typically complexes have mobilities intermediate to those of their components. We hypothesized that the mobilities of unusually high absolute values are caused by the cross-linking of virions by bivalent antibodies into aggregates with prominent side-to-side binding. Theoretically, the mobility of such aggregates should be proportional to the square root of the number of cross-linked virions. The formation of virion aggregates with prominent side-to-side binding was confirmed by atomic force microscopy. The dependence of the aggregate mobility on the number of cross-linked virions can be used to estimate this number.

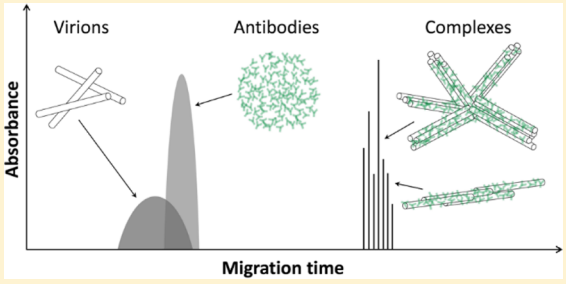

Noncovalent reversible binding of biomolecules plays an important role in cellular regulation, cell−cell recognition, bacterial and viral infections, *etc.*[1−4] Reversible binding reactions are the major component of molecular diagnostic tools such as immunoassays and hybridization assays.[5,6] In addition, most modern drugs are designed to reversibly bind their therapeutic targets.[7−9] There are multiple approaches to study noncovalent complexes; among them are biosensor-based (e.g., surface plasmon resonance and biolayer interferometry),[10,11] calorimetry based (e.g., isothermal titration calorimetry),[12] and separation-based (e.g., capillary electrophoresis (CE)) approaches.[13] Every approach is characterized by a unique set of advantages and limitations, and to some extent, different approaches complement each other. In particular, CE requires no immobilization and provides very high sensitivity for low sample consumption but is limited to species with different electrophoretic mobilities. In a typical CE migration pattern, a molecular complex has an electrophoretic mobility intermediate to those of the components it is built of. The reason for this is the approximate additivity of charges and frictional coefficients. Good examples are interactions between: proteins and proteins,[14] proteins and DNA,[15−17] and antibodies and spherical virus particles (virions).[18,19] To the best of our knowledge, deviations from this rule have not been previously reported. Here we report that the rule of intermediate electrophoretic mobility is broken for complexes of rod-like viruses with bivalent antibodies.

Virions have a variety of shapes, with the most common being spherical. Complexes of spherical virions with bivalent antibodies were studied with CE and were found to have mobilities intermediate to those of free virion and free antibody.[18,19] Some highly pathogenic viruses, including deadly Ebola[20] and Marburg[21] viruses, are spread by virions of rod-like shapes. This work was originally motivated by the fact that, while being a highly informative tool, CE has not been used to study complexes of rod-like virions with antibodies. We performed such a study using virions of Potato Virus X (PVX) and its monoclonal antibodies (Ab), both native bivalent (full-size) and monovalent derivative (Fab fragments). PVX is a plant virus that belongs to the genus *Potexvirus*, family *Alphaflexiviridae*, containing around 40 species. Potexvirus virions are flexible cylinders of various lengths (470−580 nm) and of an identical diameter of 13 nm.[22] The average molecular weight of Potexvirus virions is approximately 35,000 kDa. The RNA:protein weight ratio of virions is 6:94. Each virion contains approximately 1,300 identical coat protein subunits (8.9 subunits per turn of primary helix).

We found that the absolute values of mobilities for complexes of PVX virions with bivalent antibodies were greater than those of unbound virions and antibodies. However, the same virions with the monovalent derivative of the same antibodies did not result in complexes with greater absolute values of mobilities. We hypothesized that the deviation from the rule of complex mobilities was due to the formation of

Received: September 25, 2016
Accepted: November 8, 2016
Published: November 8, 2016

DOI: 10.1021/acs.analchem.6b03779
Anal. Chem. 2016, 88, 11908−11912

aggregates of virions cross-linked with bivalent antibodies; the monovalent antibodies cannot do such cross-linking. The theory suggests that if the aggregates are formed largely via side-by-side cross-linking, their frictional coefficient may not be proportional to the number of virions they are built of. On the contrary, the charge of the aggregate is proportional to the number of cross-linked virions. In this case, the electrophoretic mobility, which is defined as a ratio between the charge and friction coefficient, should increase in its absolute value with the growing number of cross-linked virions. We confirmed the formation of the aggregates with prominent side-to-side cross-linking of virions by atomic force microscopy (AFM) and roughly estimated the number of virions in aggregates at different molar ratios of Ab to PVX virions from the electrophoretic data.

The observed phenomenon may support an important analytical application: assessment of antibody's ability to bind virions (antigen). A greater deviation from the expected electrophoretic mobility corresponds to more virions cross-linked by the antibodies, which, in turn, corresponds to higher antigen-binding efficiency of the antibodies. The detailed analysis of electropherograms (taking into account the number of peaks as well as their heights and relative positions) can also provide semiquantitative information about the size distribution of the complexes and the approximate number of virions in a complex of a specific size. These parameters are important in vaccine development, disease diagnostics, and immunology, in general. This is especially relevant due to recent progress in the development of vaccines and viral nanoparticles based on plant viruses, in particular PVX.[23−25]

MATERIALS AND METHODS

Fused silica capillary (75 μm inner diameter, 360 μm outer diameter) was purchased from Molex (Phoenix, AZ). All chemicals were obtained from Sigma-Aldrich (Toronto, ON, Canada) unless otherwise stated. Chromeo P503 pyrylium dye was purchased from Active Motif (Burlington, ON, Canada). PVX was isolated from artificially contaminated plant leaves, and full-size bivalent monoclonal antibodies were obtained and purified as described elsewhere.[26] Purified monovalent antigen-binding fragments (Fab) were obtained from Ab using the Pierce Fab preparation kit from ThermoFisher Scientific (Waltham, MA) according to the manufacturer's instructions. The activity of Fab was confirmed by ELISA (see Supporting Information). PVX (7.4 mg/mL) was stored in phosphate buffered saline (PBS) with addition of glycerol (1:1) at −20 °C. Full-size antibodies (1.93 mg/mL) and Fab (0.6 mg/mL) were stored in PBS with addition of 0.02% NaN_3 at +4 °C. All solutions were prepared using double distilled deionized water and filtered through a 0.22 μm filter (Millipore, Nepean, ON, Canada). 50 mM Tris-HCl, pH 7.5 was used both as a run buffer and as a dilution buffer.

Capillary Electrophoresis. All CE experiments were done with a P/ACE MDQ instrument from Beckman Coulter (Fullerton, CA, U.S.) using laser-induced fluorescence (LIF) detection with excitation at 488 nm and emission at 605 nm (for Chromeo labeled virions and Ab) and light-absorption detection at 260 and 280 nm for unlabeled PVX and Ab, respectively. Uncoated fused silica capillaries of 80 cm total length and 70 cm distance from the inlet to the detection window were used for all CE experiments. New capillaries were preconditioned with 10 capillary volumes of methanol. Each run was followed by washing the capillary with 7 capillary volumes of each of 100 mM HCl, 100 mM NaOH, deionized water, and run buffer. The samples were injected by pressure at 0.5 psi (3.4 kPa) for 5 s. Capillary coolant temperature was kept at +25 °C. An electric field of 310 V/cm with a positive electrode at the injection end was applied to carry out the electrophoresis.

Chromeo P503 Labeling. 54 μL of the stock solution of antibodies was mixed with 6 μL of Chromeo P503 working solution. The obtained mixture was incubated at +4 °C for 24 h to complete the derivatization reaction, which was accompanied by a color change from blue to red. The final antibody concentration was 11.5 μM.

Atomic Force Microscopy. All AFM experiments were performed with a SmartSPM-1000 atomic force microscope (AIST-NT, Novato, CA) in a tapping mode on air using fpN01HAR cantilevers (with a tip curvature radius of 10 nm and a resonant frequency of 118−190 kHz). Dilutions of PVX and Ab were done in PBS. 10−15 μL aliquots of PVX (0.14 nM) as well as mixtures of Ab and PVX in ratios 10:1 and 50:1 were incubated for 20 min and immobilized on a freshly cleaved mica and kept for 10 min to facilitate physical adsorption of the particles on the mica surface. The excess of the liquid was carefully removed with a filter paper, and the mica was dried with an air flow. The obtained results were analyzed with Gwyddion software.[27]

RESULTS AND DISCUSSION

Separation of particles (molecules) in electrophoresis is possible due to differences in their electrophoretic mobilities μ. In turn, μ depends on the charge q and translational friction coefficient f of the particle:

$$\mu = q/f \tag{1}$$

When two particles (A and B) with different mobilities bind each other and form a complex (C), the latter typically has the mobility intermediate to those of A and B. This simple rule originates from the approximate additivities of charges and hydrodynamic sizes (the latter are directly linked with friction coefficients):

$$q_C \approx q_A + q_B, f_C \approx f_A + f_B \tag{2}$$

The mobilities of A, B, and C are then:

$$\mu_A = \frac{q_A}{f_A}, \quad \mu_B = \frac{q_B}{f_B}, \quad \mu_C \approx \frac{q_A + q_B}{f_A + f_B} \tag{3}$$

If we assume that

$$\mu_A < \mu_B \tag{4}$$

we can obtain from eqs 2 and 3 (see section 1 in the Supporting Information for the derivations) the following inequality:

$$\mu_A < \mu_C < \mu_B \tag{5}$$

Hence, in the case of additivity of charges and friction coefficients, it is expected that the mobility of a complex is intermediate to those of its components.

Our experiments with complexes of PVX virions and bivalent Ab showed a deviation from this rule. In CE, the virions and antibodies migrated as individual zones with electrophoretic mobilites close to each other (Figure 1A,B). Multiple complexes were formed by mixing bivalent antibodies with PVX virions; the complexes migrated more slowly than

DOI: 10.1021/acs.analchem.6b03779
Anal. Chem. 2016, 88, 11908−11912

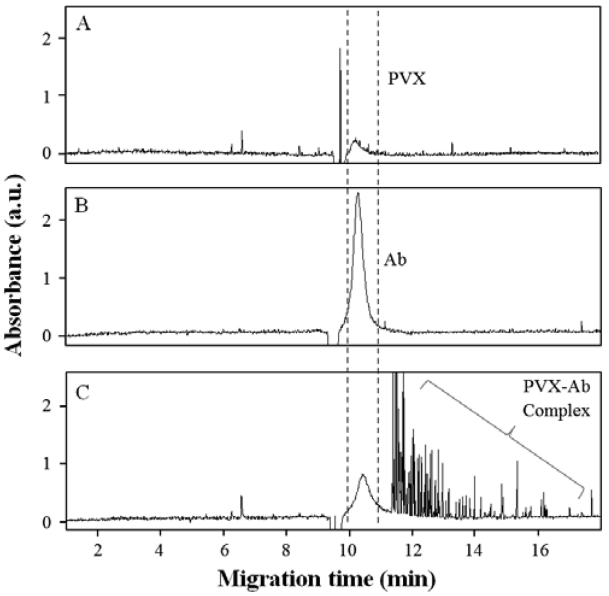

Figure 1. Migration of PVX virions, bivalent Ab, and their complexes in CE. The injected samples were: 20 nM PVX (A), 6.4 μM Ab (B), and a mixture of 20 nM PVX and 6.4 μM Ab incubated for 1 h at room temperature (C). Light absorption detection at 260 nm was used for PVX (A) and at 280 nm for Ab and the PVX-Ab mixture (B, C). The dotted lines flank the region of migration of unbound PVX and Ab.

unbound virions and antibodies (Figure 1C), which is equivalent to complexes having greater absolute values of electrophoretic mobilities. Unbound antibodies and virions as well as their complexes migrate slower than the electroosmotic flow (marked by a peak with negative absorbance at ~9.5 min) and, thus, have negative electrophoretic mobilities. This allows us to operate with absolute values of mobilities through the rest of this paper. We confirmed that the observed set of multiple peaks was not a result of virion disruption, but corresponded to complexes between the virions and bivalent antibodies, by performing similar CE experiments with Chromeo P503 labeled antibodies and LIF rather than light-absorbance detection (see section 2 in the Supporting Information). In this case, only free antibodies and antibody-containing complexes were detected.

When PVX virions were mixed with the monovalent Fab fragments, the complexes could not be separated from unbound virions and antibodies and, thus, had mobilities similar to those of unbound virions and antibodies (see section 3 in the Supporting Information).

To explain the anomalous mobility of the complexes between the virions and bivalent antibodies, we hypothesized that bivalent antibodies cross-link virions into aggregates with disproportionally small friction coefficients. Such aggregates should have significant side-by-side cross-linking of virions with cylinder-like shape of the aggregates (Figure 2). Individual virions and their aggregates can be considered as cylinders with different diameters.

We can theoretically estimate how the mobility of cylindrical aggregates depends on the number (n) of cross-linked particles. The antibodies play a role of "staples" connecting the virions and are, thus, sufficient in a relatively small molar excess to the virions. In addition, the antibodies are much smaller than the virions. Accordingly, both the charge and mobility of the aggregates will be defined by the corresponding parameters of

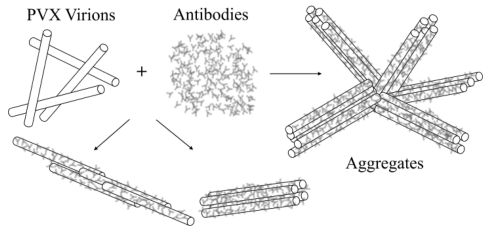

Figure 2. Schematic illustration of formation of near-cylindrical aggregates of rod-like virions cross-linked side-by-side via bivalent antibodies.

the virions. The charge of the aggregate is a sum of the charges of individual virions it is built of. For similar virions, the charge of the aggregate (q_{agg}) is proportional to the number of the cross-linked virions and the charge of a single virion (q_{vir}):

$$q_{agg} \approx nq_{vir} \tag{6}$$

On the contrary, the friction coefficient is a nonadditive function in this case, even in the first approximation. The friction coefficient is proportional to the surface area of the particle (A_{cyl}), which, for a cylindrical aggregate (see Figure 2), is proportional to $n^{1/2}$, as shown in the following:

$$f_{agg} \sim A_{cyl} \approx \frac{1}{2}\pi d_{agg}^{\ 2} + \pi L d_{agg} \approx \frac{1}{2}\pi n d_{vir}^{\ 2} + \pi L d_{vir} n^{1/2} \approx \pi L d_{vir} n^{1/2} \tag{7}$$

Here L is the length of the cylinder and d_{agg} and d_{vir} are the diameters of its base for the aggregate and the individual virion, respectively. In the last step of the derivations, we neglected the area of the cylinder base in the assumption that the cylinder length (around 500 nm) is much greater than its diameter (13 nm): $L \gg d_{vir}$. Also, d_{agg} is proportional to $n^{1/2}d_{vir}$.

By using eqs 1, 6, and 7, we can obtain a relation between the electrophoretic mobility and the number of virions in the cylindrical aggregate:

$$\mu_{agg} \sim \frac{nq}{n^{1/2}\pi L d_{vir}} = n^{1/2}\frac{q}{\pi L d_{vir}} \tag{8}$$

Thus, the absolute value of the electrophoretic mobility should grow with the number of cross-linked virions proportionally to a square root of n. Since $q/(\pi L d_{vir})$ is proportional to the mobility of an individual virion (μ_{vir}), we can write

$$\mu_{agg} \approx n^{1/2}\mu_{vir} \tag{9}$$

Accordingly, complex mobility in this case can be used to estimate roughly the number of cross-linked virions:

$$n \approx (\mu_{agg}/\mu_{vir})^2 \tag{10}$$

To estimate n for aggregates of PVX virions, we determined the values of μ for free virions and for all of the aggregates at different ratios of full-size antibody:PVX virion (see section 4 in the Supporting Information) and plotted the normalized peak intensity of each fraction as a function of the number of virions (Figure 3). Expectedly, the number of cross-linked virions in aggregates grew with the antibody concentration. The heterogeneity of sizes also increased with increasing concentration of antibodies.

We then used AFM imaging to confirm the formation of aggregates with prominent side-to-side cross-linking of virions by bivalent antibodies. In the absence of antibodies, we

DOI: 10.1021/acs.analchem.6b03779
Anal. Chem. 2016, 88, 11908−11912

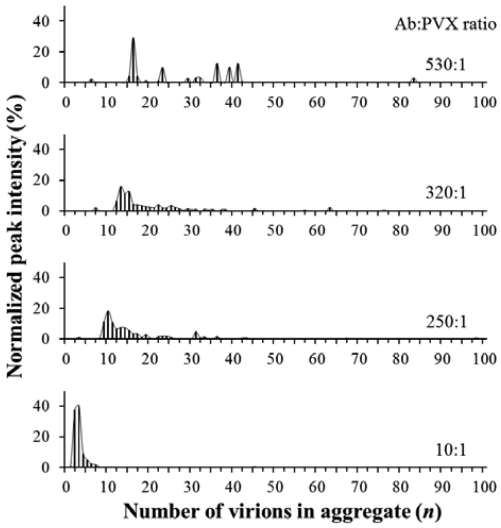

Figure 3. Influence of the molar ratio Ab:PVX on the size distribution of aggregates of PVX virions cross-linked with bivalent antibodies. Bars represent fraction distribution profiles of aggregates at different Ab:PVX ratios. The solid line on top shows the same data in a curve form.

observed individual virions of the expected dimensions (Figure 4A). In the presence of a molar excess of antibodies, we found

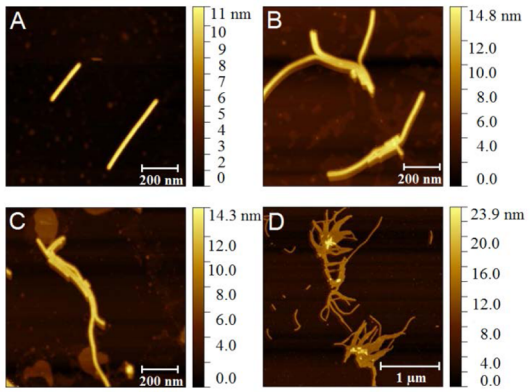

Figure 4. AFM images of individual PVX virions (A) and their full-size antibody-cross-linked aggregates of different sizes (B–D). Image A was obtained in the absence of antibodies. The molar ratios of antibodies to virions used to obtain images B and C were 10, and for image D it was 50. The color scale is to indicate the height profile of the structures in the image.

aggregates with prominent side-to-side cross-linking. Even a 10-time molar ratio between the antibodies and virions was sufficient for aggregate formation (Figure 4B). Further increase in this ratio led to the formation of larger branching clusters of aggregates still with a significant content of side-to-side binding (Figure 4C).

When virions were mixed with monovalent Fab fragments, no aggregate formation was observed by AFM, thus confirming the cross-linking nature of aggregate formation in the case of bivalent antibodies.

AFM results also showed that the aggregates of PVX virions cross-linked by bivalent antibodies grew not only in their diameter but also in their length (Figure 4B). The elongation was due to the expected partial overlap of cross-linked virions. Importantly, such elongation can further increase the absolute value of electrophoretic mobility if the aggregate retains near-linear shape. The elongation will increase the dipole moment of the particle and lead to more pronounced orientation of the particle along the electric field and thus along the direction of its translational movement. Such orientation will, in turn, lead to decreasing effective translational friction coefficient and, accordingly, increasing electrophoretic mobility. This hypothetical explanation is strongly supported by the previously observed increase of absolute electrophoretic mobility with increasing length of single-walled carbon nanotubes.[28] The increase of the absolute value of the electrophoretic mobility with greater extent of particle orientation along the direction of translational movement was also reported for rod-like viruses.[29] Thus, even for elongated aggregates, we can still expect absolute values of electrophoretic mobilities greater than that of individual virions. The increased mobility will be characteristic also for clusters of aggregates shown in Figure 3C.

CONCLUSIONS

In this work, we report on the high absolute electrophoretic mobility of complexes of rod-like virions with bivalent antibodies. The behavior is explained by the formation of cross-linked aggregates of virions in which the charge is proportional to the number of cross-linked virions but the friction coefficient is roughly proportional to the square root of this number. Accordingly, electrophoretic mobility is roughly proportional to the square root of the number of cross-linked virions. The formation of aggregates is clearly seen with AFM and is restricted to complexes of virions with bivalent antibodies; the complexes of virions with monovalent antibodies do not form the aggregates. The larger absolute value of the electrophoretic mobility of the aggregates makes it possible to separate them from the unbound virions and antibodies by CE. This, in turn, can potentially facilitate kinetic and thermodynamic studies of complex formation between the rod-like viruses and antibodies.

ASSOCIATED CONTENT

Supporting Information

The Supporting Information is available free of charge on the ACS Publications website at DOI: 10.1021/acs.analchem.6b03779.

Derivation of inequality for the electrophoretic mobility of the complex; CE experiments with Chromeo P503-labeled antibodies; investigation of the mixtures containing virions and monovalent antigen-binding fragments; estimation of the approximate number of virions (n) in aggregates; and a reference (PDF)

AUTHOR INFORMATION

Corresponding Author

*E-mail: skrylov@yorku.ca.

ORCID

Sergey N. Krylov: 0000-0003-3270-2130

Notes

The authors declare no competing financial interest.

ACKNOWLEDGMENTS

The work of the York University team was supported by the Natural Sciences and Engineering Research Council of Canada (grants STPGP 463455 and 449140-2014). The work of the

DOI: 10.1021/acs.analchem.6b03779
Anal. Chem. 2016, 88, 11908–11912

Russian Academy of Sciences team was supported by the Russian Science Foundation (grant 14-16-00149).

REFERENCES

(1) Liu, S.; Thomas, S. M.; Woodside, D. G.; Rose, D. M.; Kiosses, W. B.; Pfaff, M.; Ginsberg, M. H. *Nature* **1999**, *402*, 676−681.
(2) Butcher, E. C. *Cell* **1991**, *67*, 1033−1036.
(3) Aderem, A.; Ulevitch, R. J. *Nature* **2000**, *406*, 782−787.
(4) Sauter, N. K.; Hanson, J. E.; Glick, G. D.; Brown, J. H.; Crowther, R. L.; Park, S. J.; Skehel, J. J.; Wiley, D. C. *Biochemistry* **1992**, *31*, 9609−9621.
(5) Liu, S.; Zhang, X.; Wu, Y.; Tu, Y.; He, L. *Clin. Chim. Acta* **2008**, *395*, 51−56.
(6) Wegman, D. W.; Krylov, S. N. *Angew. Chem., Int. Ed.* **2011**, *50*, 10335−10339.
(7) Shieh, Y. A.; Yang, S. J.; Wei, M. F.; Shieh, M. J. *ACS Nano* **2010**, *4*, 1433−1442.
(8) Flego, M.; Ascione, A.; Cianfriglia, M.; Vella, S. *BMC Med.* **2013**, *11*, 4.
(9) Saylor, C.; Dadachova, E.; Casadevall, A. *Vaccine* **2009**, *27*, G38−G46.
(10) Urusov, A. E.; Kostenko, S. N.; Sveshnikov, P. G.; Zherdev, A. V.; Dzantiev, B. B. *Sens. Actuators, B* **2011**, *156*, 343−349.
(11) Hong, M.; Lee, P. S.; Hoffman, R. M. B.; Zhu, X.; Krause, J. C.; Laursen, N. S.; Yoon, S.-I.; Song, L.; Tussey, L.; Crowe, J. E.; Ward, A. B.; Wilson, I. A. *J. Virol.* **2013**, *87*, 12471−12480.
(12) Weber, P. C.; Salemme, F. R. *Curr. Opin. Struct. Biol.* **2003**, *13*, 115−21.
(13) Kanoatov, M.; Galievsky, V. A.; Krylova, S. M.; Cherney, L. T.; Jankowski, H. K.; Krylov, S. N. *Anal. Chem.* **2015**, *87*, 3099−3106.
(14) Chu, Y.-H.; Lees, W. J.; Stassinopoulos, A.; Walsh, C. T. *Biochemistry* **1994**, *33*, 10616−10621.
(15) Bao, J.; Krylova, S. M.; Cherney, L. T.; Hale, R. L.; Belyanskaya, S. L.; Chiu, C. H.; Arico-Muendel, C. C.; Krylov, S. N. *Anal. Chem.* **2015**, *87*, 2474−2479.
(16) De Jong, S.; Krylov, S. N. *Anal. Chem.* **2011**, *83*, 6330−6335.
(17) Krylova, S. M.; Karkhanina, A. A.; Musheev, M. U.; Bagg, E. A.; Schofield, C. J.; Krylov, S. N. *Anal. Biochem.* **2011**, *414*, 261−265.
(18) Okun, V. M.; Ronacher, B.; Blaas, D.; Kenndler, E. *Anal. Chem.* **2000**, *72*, 4634−4639.
(19) Okun, V. M.; Moser, R.; Blaas, D.; Kenndler, E. *Anal. Chem.* **2001**, *73*, 3900−3906.
(20) Kiley, M. P.; Regnery, R. L.; Johnson, K. M. *J. Gen. Virol.* **1980**, *49*, 333−341.
(21) Geisbert, T. W.; Jahrling, P. B. *Virus Res.* **1995**, *39*, 129−150.
(22) Atabekov, J.; Dobrov, E.; Karpova, O.; Rodionova, N. *Mol. Plant Pathol.* **2007**, *8*, 667−675.
(23) Wen, A. M.; Steinmetz, N. F. *Chem. Soc. Rev.* **2016**, *45*, 4074−4126.
(24) Uhde-Holzem, K.; McBurney, M.; Tiu, B. D.; Advincula, R. C.; Fisher, R.; Commandeur, U.; Steinmetz, N. F. *Macromol. Biosci.* **2016**, *16*, 231−241.
(25) Lico, C.; Benvenuto, E.; Baschieri, S. *Front. Plant Sci.* **2015**, *6*, 1009.
(26) Safenkova, I. V.; Zherdev, A. V.; Dzantiev, B. B. *J. Immunol. Methods* **2010**, *357*, 17−25.
(27) Nečas, D.; Klapetek, P. *Cent. Eur. J. Phys.* **2012**, *10*, 181−188.
(28) Doorn, S. K.; Fields, R. E.; Hu, H.; Hamon, M. A.; Haddon, R. C.; Selegue, J. P.; Majidi, V. *J. Am. Chem. Soc.* **2002**, *124*, 3169−3174.
(29) Grossman, P. D.; Soane, D. S. *Anal. Chem.* **1990**, *62*, 1592−1596.

DOI: 10.1021/acs.analchem.6b03779
Anal. Chem. 2016, 88, 11908−11912

Supporting Information

UNEXPECTEDLY-HIGH ELECTROPHORETIC MOBILITY OF COMPLEXES BETWEEN ROD-LIKE VIRIONS AND BIVALENT ANTIBODIES

Stanislav S. Beloborodov,[1] Vasily G. Panferov,[2] Irina V. Safenkova,[2] Svetlana M. Krylova,[1] Boris B. Dzantiev,[2] and Sergey N. Krylov,[1]

[1]*Department of Chemistry, York University, Toronto, ON, Canada*

[2]*Russian Academy of Sciences, A.N. Bach Institute of Biochemistry, Moscow, Russian Federation*

Table of Contents

1. Derivation of inequality for electrophoretic mobility of the complex

To obtain inequality (5) in main text, we rewrite inequality $\mu_A < \mu_B$ in a following manner:

$$\frac{q_A}{f_A} < \frac{q_B}{f_B} \quad \text{(S1)}$$

$$q_A f_B < q_B f_A \quad \text{(S2)}$$

By adding $q_A f_A$ to both sides in (S2) we get:

$$q_A f_B + q_A f_A < q_B f_A + q_A f_A \quad \text{(S3)}$$

$$q_A (f_B + f_A) < f_A (q_B + q_A) \quad \text{(S4)}$$

$$\frac{q_A}{f_A} < \frac{(q_B + q_A)}{(f_B + f_A)} \quad \text{(S5)}$$

By adding $q_B f_B$ to both sides in (S2) we get:

$$q_A f_B + q_B f_B < q_B f_A + q_B f_B \quad \text{(S6)}$$

$$f_B (q_A + q_B) < q_B (f_A + f_B) \quad \text{(S7)}$$

$$\frac{(q_B + q_A)}{(f_B + f_A)} < \frac{q_B}{f_B} \quad \text{(S8)}$$

By combining (S5) and (S8) we get:

$$\frac{q_A}{f_A} < \frac{(q_B + q_A)}{(f_B + f_A)} < \frac{q_B}{f_B} \quad \text{(S8)}$$

or

$$\mu_A < \mu_C < \mu_B \quad \text{(S9)}$$

2. CE experiments with Chromeo P503-labeled antibodies

To confirm the formation of multiple complexes and their atypical migration we performed a number of CE experiments with Chromeo P503 labeled antibodies. It was found that the labeled antibodies, being analyzed separately, formed two peaks on an electropherogram (**Supporting Figure 1**, lower traces). Upon adding the virions, the higher peak did not change, but the smaller one decreased its height (the decrease was more pronounced at a 100:1 Ab:PVX ratio (**Supporting Figure 1-B**) than at a 1000:1 ratio (**Supporting Figure 1-A**)). Accordingly, the higher peak was assigned either to the fluorescently labeled small-molecule products of the Ab deamidation[1] or to the external contaminant, and the smaller one to the fluorescently labeled antibodies by itself.

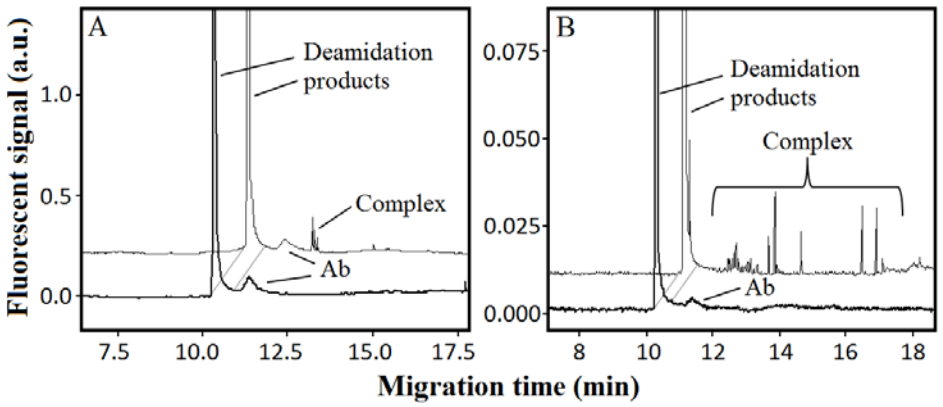

Supporting Figure 1. CE-LIF analysis of mixtures of Chromeo P503 labeled antibodies (Ab) and unlabeled virus at different antibody:virions ratios: 1000:1 (A) and 100:1 (B). The bottom traces correspond to Ab-only controls (at 1 μM and 100 nM concentrations, respectively). For clarity of presentation, a time offset of 1 min and signal offsets of 0.25 (A) and 0.01 (B) units were applied. LIF detection was at 605 nm.

3. Investigation of the mixtures containing virions and monovalent antigen-binding fragments

As a negative control in our CE experiments we used monovalent fragments (Fab) of original bivalent monoclonal antibodies (Ab). Fab is unable to cross-bind viral particles. We found that the complex of virions with Fab migrated as a uniform zone and resulted in a single peak on the electropherogram. The mobility of this complex was equal to that of the virion within the limits of experimental error (**Supporting Figure 2**).

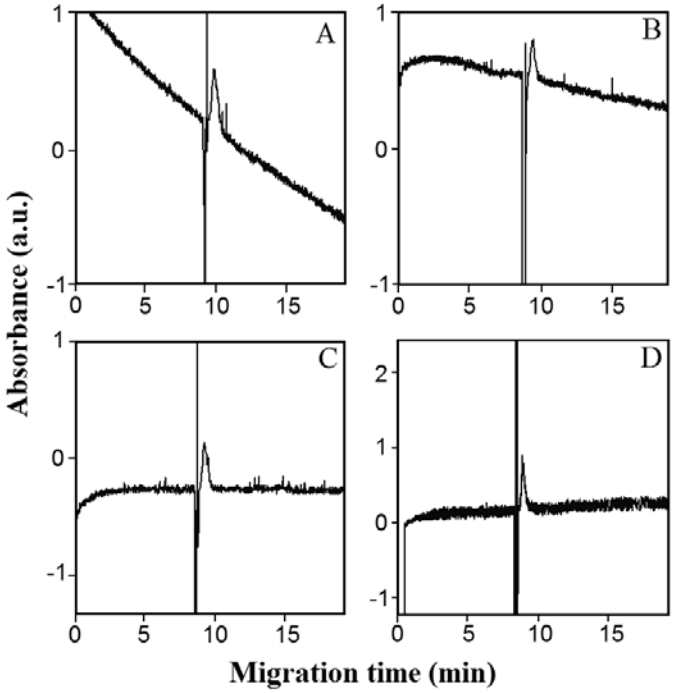

Supporting Figure 2. Detection of 63 nM PVX in the presence of monovalent antibodies (Fab) at 260 nm. (A) represents PVX only; (B) represents Fab:PVX in a ratio of 2:1; (C) represents Fab:PVX in a ratio of 10:1; (D) represents Fab:PVX in a ratio of 135:1. Absorbance at 260 nm.

To confirm the antigen-binding ability of obtained Fab we performed ELISA. Nondigested IgG was used as a positive control. Microplate wells were filled with 100 μL solution of PVX in PBS (1 μg/ml) and incubated at 37 °C for 2 h to complete the immobilization. The microplate was washed four times with a mixture of PBS and 0.05% Triton X-100 (PBST). Series of dilutions of Ab (2.00, 1.00, 0.500, 0.250, 0.125, 0.063, 0.031, 0.017 μg/mL) and Fab (5.00, 2.50, 1.25, 0.625, 0.313, 0.156, 0.078, 0.039 μg/mL) were added to immobilized virions and incubated at 37 °C for 1 hour followed by washing procedure that described above. Then portions of secondary antibodies conjugated with peroxidase were added to the wells and incubated at 37°C for 1 h followed by washing. To determine the peroxidase activity, the substrate solution (100 mL of 0.4 mM 3,3′,5,5′-tetramethyl-benzidine solution in 40 mM sodium citrate buffer, pH 4.0, containing 3 mM H_2O_2) was added to each microplate well and incubated for 15 min at room temperature. Then reaction was terminated by adding 1 M H_2SO_4 (50 mL) and optical density

measurements were conducted using EnSpire Multimode Plate Reader at 450 nm wavelength (room temperature). Each sample was studied in triplicates. The statistical treatment was done by Origin Pro 9.0 (Origin Lab, Northampton, MA, USA). Results showed that produced Fab fragments are able to bind virus particles (**Supporting Figure 3**).

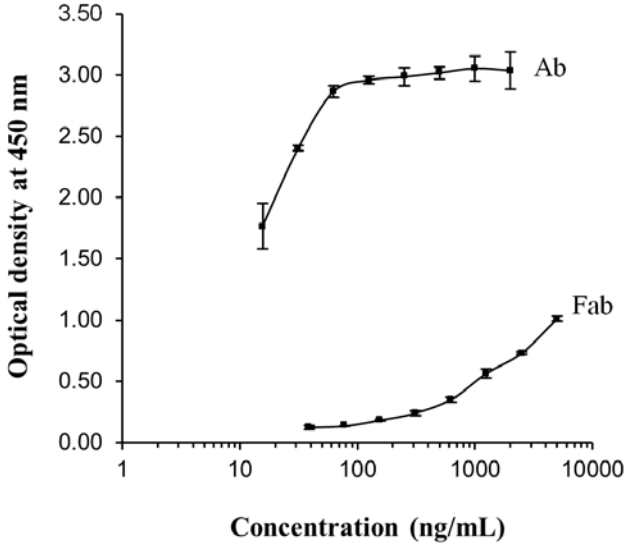

Supporting Figure 3. Optical density of Ab and Fab solutions as a function of their concentrations (in logarithmic scale). As follows from the graph, the binding activity of Ab is higher than that for Fab. It can be explained by the fact, that fragmentation (hydrolysis) of a parent antibody (Ab) to Fab leads to the loss of antigenic determinants that can be recognized by secondary antibody (located in the Fc region), which decreases the amount of Fab-secondary antibody interactions. Increasing Fab concentration leads to an increase in the optical density of the solution, which confirms the remaining of their functional activity (the ability to bind PVX).

4. Estimation of the approximate number of virions (*n*) in aggregates

We performed a set of CE experiments (light-absorption detection at 280 nm) with PVX solutions (20 nM concentration) and mixtures containing Ab and PVX in different ratios in order to measure the electrophoretic mobilities (μ) of the virions and complexes. The values for mobilities were then used to estimate the number of virions (n) in the aggregates (formula 9, main text).

Ab-PVX mixtures were obtained by mixing the antibodies (at a constant concentration of 6.4 μM) with different concentrations of PVX virions (12, 20 and 25 nM), which gave us three solutions of different Ab:PVX ratios: 530:1, 320:1 and 250:1. The mixture with 10:1 ratio was obtained by mixing 420 nM antibodies with 42 nM PVX. Prior to each CE injection we spiked the samples (virions by themselves, as well as the mixtures) with 10 mM DMSO (detection at 214 nm) which served as a marker of electroosmotic flow. The electroosmotic mobility then was calculated by the following formula:

$$\mu_{\mathrm{EOF}} = \frac{L}{t_{\mathrm{DMSO}}} \times \frac{L_{\mathrm{t}}}{V} \qquad (1)$$

where μ_{EOF} is electroosmotic mobility ($\mathrm{cm^2/V \cdot min}$), L is a distance from the capillary inlet to the detection window (71.9 cm), t_{DMSO} is an average migration time of DMSO (min); L_{t} is a total length of the capillary (82.2 cm) and V is an applied voltage (25 kV). The obtained value of μ_{EOF} was then used for calculation of the absolute values of negative electrophoretic mobilities of the virions and aggregates:

$$\mu = \mu_{\mathrm{EOF}} - \frac{L}{t_{\mathrm{mig}}} \times \frac{L_{\mathrm{t}}}{V} \qquad (2)$$

Here t_{mig} is a migration time of the PVX or aggregates. In a case of aggregates (complexes) we used t_{mig} for each individual peak (fraction) to calculate μ and n. Then, we calculated the normalized peak intensity (%) for individual fractions as a ratio between the average value of intensity (a.u.) of the chosen peak and the total average sum of intensities (a.u.) for all of the peaks that belong to aggregates (based on the data of two experiments for each of the PVX:Ab ratios). Further, we plotted the normalized peak intensity (%) as a function of the integer values of n in a range of 0, 1, 2…100 (main text, **Figure 3).** Such a pattern can be considered as a fraction distribution profile for each of the Ab:PVX ratios, where the

normalized peak intensity is proportional to the relative concentration of the fraction with chosen *n* (in approximation that the full width at half maximum for all of the peaks is same)

5. Reference

(1) Wang, W.; Meeler, A. R.; Bergerud, L. T.; Hesselberg, M.; Byrne, M.; Wu, Z. *Int. J. Mass Spectrom.* **2012**, *312*, 107-113.